

Automatika

Journal for Control, Measurement, Electronics, Computing and Communications



ISSN: (Print) (Online) Journal homepage: www.tandfonline.com/journals/taut20

Removal of salt and pepper noise using adaptive switching modified decision-based unsymmetric trimmed median filter optimized with Hyb-BCO-FBIA

S. Mohan & B. Paulchamy

To cite this article: S. Mohan & B. Paulchamy (2024) Removal of salt and pepper noise using adaptive switching modified decision-based unsymmetric trimmed median filter optimized with Hyb-BCO-FBIA, *Automatika*, 65:3, 852-865, DOI: [10.1080/00051144.2024.2321807](https://doi.org/10.1080/00051144.2024.2321807)

To link to this article: <https://doi.org/10.1080/00051144.2024.2321807>



© 2024 The Author(s). Published by Informa UK Limited, trading as Taylor & Francis Group.



Published online: 26 Feb 2024.



[Submit your article to this journal](#)



Article views: 356



[View related articles](#)



[View Crossmark data](#)



Removal of salt and pepper noise using adaptive switching modified decision-based unsymmetric trimmed median filter optimized with Hyb-BCO-FBIA

S. Mohan^a and B. Paulchamy^b

^aDepartment of Electronics and Communication Engineering, Nehru Institute of Engineering and Technology, Coimbatore, Tamilnadu, India; ^bDepartment of Electronics and Communication Engineering, Hindusthan Institute of Technology, Coimbatore, Tamilnadu, India

ABSTRACT

An intriguing area in the IP (image processing) is the recovery of noisy photographs from the noise caused by the salt and pepper. As the mistake rate rises and the image format varies, the issue with the current task does not go away. In this study, Salt and Pepper Denoising, Hybrid Balancing Composite motion Optimization with Adaptive Switching Modified Decision based Unsymmetric Trimmed Median Filter and Forensics-Based Investigation Algorithm is proposed (R-SPN-ASMD-UTMF-Hyb-BCO-FBIA). Initially, the input images are obtained from boat-types-recognition dataset, cat-breeds-dataset, cars-image-dataset, butterfly-images 40-species dataset and birds-200 dataset. The images are pre-processed through an ASMD-UTMF filter. ASMD-UTMF does not expose any adoption of optimization systems to calculate the optimal parameters. Therefore, the proposed Hyb-BCO-FBIA is employed for optimizing the ASMD-UTMF weight parameters. The suggested system is implemented on MATLAB and the assessment metrics as Mean Square Error (MSE), Structural similarity index measurement (SSIM), Peak signal to noise ratio (PSNR), Normalized cross-correlation (NC), Image Enhancement Factor (IEF), Mean Square Error (MSE) are analysed. The proposed method attains higher PSNR, NC related with other SOTA (State-Of-The Art) methods.

ARTICLE HISTORY

Received 27 October 2023
Accepted 16 February 2024

KEYWORDS

Adaptive switching modified decision based unsymmetric trimmed median filter; balancing composite motion optimization; forensic-based investigation algorithm; salt and pepper noise

1. Introduction

In the digital world, a general difficulty is that images with noise are degraded during transmitting, receiving and storage periods. There are several noises acquired in the images particularly SPN (Salt and Pepper Noise), which alters grey values and affects the pixels of the images so it does not show the grey values to the nearby locality [1]. These noises are caused due to the error that occurs in the transmission channel or noisy sensors. Generally, the SPN is reduced through their high energy and small duration of impulse noise [2]. There are several approaches employed for removing the SPN from the pictures. There are two main techniques in the removal of noise. One is a linear filter and the other is a non-linear filter. A linear filter (LF) is used for blurring the images and a non-linear filter (NLF) is used to remove the noise [3]. A small amount of noisy pixels is replaced through the median value at a low density of noise but it fails to replace with a higher density of noise because it needs a larger window size to degrade the noise. Hence the correlation between the replaced and noisy median values is less compared to the low density of pixels. In this technique, the corrupted pixels are replaced with the median pixel values of a filtering window, which finds out the nearby locality of pixels

by keeping the filtering window size fixed to calculate a median intensity level for replacing the pixel value. Image noise removal has been taken as a significant task in image processing. During the pre-processing stage in the IP, image denoising may look after edges, textures, and other image details [4]. SAP noise generally exists on natural images, and pixels contaminated by SAP noise take the maximal or minimal value that may be denoted from black or white points.

To eliminate Salt-and-Pepper noise, many computational systems have been presented. These filtering techniques may restore image detail well at low noise intensity, but execute poorly at high noise intensity. As a result, the earlier strategies raised the rate of mistakes and failed to achieve sufficient efficiency by removing salt and pepper noise in the original image, which motivated us to carry out this work.

In this manuscript, the removal of salt and pepper noise with ASMD-UTMF optimized with hybrid balancing composite motion optimization and a forensic-based investigation algorithm is proposed. Initially, the input images are taken from the boat-types-recognition dataset, cat-breeds-dataset, cars-image-dataset, butterfly-images40-species dataset and birds-200 dataset. The images received from the data centre

CONTACT S. Mohan ✉ smohan2507@gmail.com 📍 Department of Electronics and Communication Engineering, Nehru Institute of Engineering and Technology, Coimbatore, Tamilnadu, 641105, India

© 2024 The Author(s). Published by Informa UK Limited, trading as Taylor & Francis Group.

This is an Open Access article distributed under the terms of the Creative Commons Attribution-NonCommercial License (<http://creativecommons.org/licenses/by-nc/4.0/>), which permits unrestricted non-commercial use, distribution, and reproduction in any medium, provided the original work is properly cited. The terms on which this article has been published allow the posting of the Accepted Manuscript in a repository by the author(s) or with their consent.

contain an excess of salt and pepper noise, hence it is filtered using the ASMD-UTMF filter. Generally, the ASMD-UTMF filter is unable to expose any adoption of optimization systems for computing the optimal parameters for decreasing the SPN inside the filtered image. Therefore, proposed Hyb-BCO-FBIA to optimize the weight parameters of the ASMD-UTMF. The important contribution of this manuscript is summarized below,

- In this manuscript, the removal of salt and pepper noise with ASMD-UTMF optimized with hybrid balancing composite motion optimization and a forensic-based investigation algorithm is proposed (RSP-ASMD-UTMF-Hyb-BCO-FBIA).
- Initially, the input images are taken from the boat-types-recognition dataset, cat-breeds-dataset, cars-image-dataset, butterfly-images40-species dataset and birds-200 dataset.
- The images received from the data centre contain an excess of SPN, and hence it is pre-processed using ASMD-UTMF [5].
- Therefore, the proposed hybrid balancing composite motion optimization [6] and forensic-based investigation algorithm [7] (Hyb-BCO-FBIA) was utilized to optimize the weight parameters of the ASMD-UTMF.
- The suggested system is implemented on MATLAB and assessment metrics such as PSNR, SSIM and NC, MSE, and IEF are analysed.
- In terms of de-noising images in the SPN using hybrid filters, fuzzy logic noise detectors, and genetic optimization algorithms (RSPN-HFGOA, RSPN-ANFIS, RSPN-APCNN-GWO, and RSPN-DB-ATMWMF, respectively), the effectiveness of the suggested RSP-ASMD-UTMF-Hyb-BCO-FBIA method is compared to the current systems.

The remaining manuscript has been designed to be. The literature review is presented in Section 2, the proposed methodology is presented in Section 3, the results and discussions are provided in Section 4, and the manuscript is concluded in Section 5.

2. Related works

This section evaluated some of the most recent studies conducted on the reduction of SPN.

Senthilselvi et al. [8] have presented an Adaptive Neuro-Fuzzy System (ANFIS) on top of a Fuzzy Inference System (FIS) with an optimization algorithm to denoise images from SPN. The suggested network is utilized to get dissimilar patterns of noisy pixels. It provides a higher PSNR with a lower image enhancement factor.

Kiruban et al. [9] have presented the removal of SPN with an optimized Adaptive Pulse-Coupled Neural

Network (APCNN) under the Shearlet Transform (ST) domain. At the ST domain, PCNN improves the delicacy of imageries under low and high recurrence sub-bands. The high and low recurrence enhanced sub-bands were used for inverse ST to obtain enhanced images. It provides improved PSNR value with minimal SSIM.

Christo et al. [10] have presented a decision that depends on an asymmetrically trimmed modified winsorized MF for the removal of SPN on images. The presented filter originally classifies pixels as noisy and non-noisy with an asymmetrically clipped modified winsorized median, leaving the non-noisy pixels. Extensive analyses were performed on a standard image database and the performance of the suggested filter was assessed in quantitative and qualitative terms. It provides a lower image enhancement factor with a higher PSNR value.

Sharma et al. [11] have presented an iterative multi-layer decision-based filter to remove SPN. In this case, efficient decisions depend on the noise density of the image utilized. A fixed-size window was utilized at every step to preserve maximal correlation all over the filtering process. The pre-edge and post-aliasing processing was also featured to improve image quality. It provides high reverse noise density with lower PSNR values.

Zhang et al. [12] have presented a non-local adaptive mean filter (NAMF) to remove salt and pepper noise. The noisy pixel was then replaced through the combination of their neighbouring pixels, and lastly, a non-local mean filter depends on salt and pepper noise was utilized to recreate the intensity values of the noisy pixels. It does not provide better performance based on the feature for restoring imageries at the entire SAP noise levels, but it does provide a high PSNR value.

3. Proposed methodology

In this manuscript, the elimination of SPN with ASMD-UTMF optimized with hybrid balancing composite motion optimization and a forensic-based investigation algorithm is suggested. The block diagram of the suggested RSPN-ASMD-UTMF-Hyb-BCO-FBIA method is given in Figure 1. The comprehensive discussion about the removal of salt and pepper noise with ASMD-UTMF optimized with Hyb-BCO-FBIA algorithm is given below,

3.1. Image acquisition

Initially, the input images like boat-ocean-sea-water-sunset, boat-sea-inflatable-boat-coast, and ferry-cargo-ship-carrier-the-barge-venic are taken from the boat-types-recognition dataset. Cat-image-Domestic Long Hair, cat-image-Maine Coon and cat-image-Siberian are taken from the cat-breeds-dataset. Car-road-Audi, img-road-Hyundai Creta, img-road-Toyota Innova are

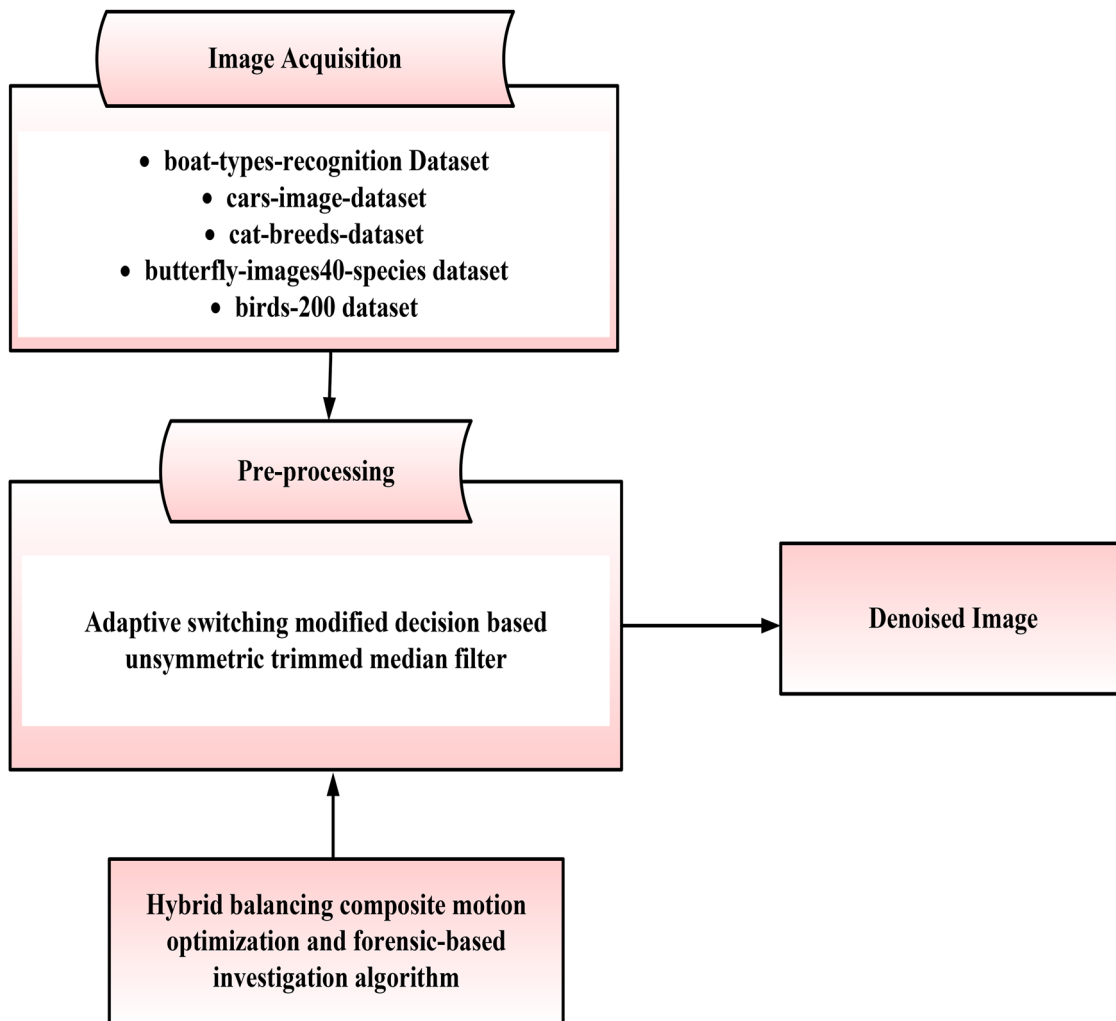


Figure 1. Block diagram of proposed RSPN-ASMD-UTMF-Hyb-BCO-FBIA method.

from cars-image-dataset. Butterfly-plant-img-ATALA, butterfly-plant-img-RED CRACKER, butterfly-plant-img-ORANGE TIP are taken from butterfly-images40-species dataset and girl-people-landscape-sun, Yellow-bellied-Flycatcher and bird-photo-Flamingo are taken from birds-200 dataset.

3.2. Preprocessing with adaptive switching modified decision-based unsymmetric trimmed median filter

The input images contain an excess of SPNs, in order to eliminate noises as input images and to increase the quality of the image ASMD-UTMF is proposed. The noisy detection process can be done with the identification of Local Intensity Fluctuation (LIF) of salt and pepper noise (SPN). It shows their structure as extensively darker, extensively brighter, single or isolated dots contrast with other nearby pixels and hence the corrupted pixels are considered as intensity function of local extrema (LIE). If the pixels are brighter than their nearby pixels which are said to be a Local Intensity Maxima (LIM_{max}) or else if the pixels are darker than their nearby pixels which are said to be

a Local Intensity Minima (LIM_{min}). Initially, it looks for LIE for the purpose of deciding whether the pixels of images are uncorrupted or corrupted. The exploration process is defined by the square window because it passes through pixel by pixel in the image. Every window LIM_{max} and LIM_{min} intensity location are defined and marked by local extrema map for enhancing the corresponding values. For instance, the size of the window is considered as $n \times n$ pixels, all pixels in the window are regarded as LIE of n^2 times and the values of extrema on the map are assumed as “the strength of the extremum”. The number of times the pixel was identified as an extremum in the selected neighbourhood when the extremum is stronger. The pixel is considered a noisy pixel when n^2 number of times it appears in the local extremum window. Particularly n^2 value identifies and locates the light dot (salt noise) in the maxima map. Similarly, n^2 value identifies and locates the dark dot (pepper noise) in the minima map. To remove high-density noise as specified input images, all pixels in size window are built of noisy pixels. The render pixel is checked whether it is noisy or not. If the value of the processing pixel is among the minimal “1” and the maximal “254”. If the value of the processing pixel is 0 or

255, then it is a noisy pixel that is managed through the suggested ASMD-UTMF technique.

The appearance of high-density noise on input images results from 0 or 255 in noisy pixels linked to pepper and salt types of noise in Equation (1).

$$S = \{0, a, 255\} \quad (1)$$

From Equation (1), $a \in [1, 254]$ and then the noisy pixels are recognized depending on Equation (2),

$$Nq^{ab} = \begin{cases} 1, & \text{if } q^{ab} = 0; \\ 1, & \text{if } q^{ab} = R; \\ 0, & \text{if } q^{ab} >= 1 \ \&\& \ q^{ab} <= R - 1; \end{cases} \quad (2)$$

where Nq^{ab} represents the noisy pixels, R indicates the maximal grey level, $a \in [0, \text{ImageHeight} - 1]$ and $b \in [0, \text{ImageWidth} - 1]$. Based on Equation (2), if Nq^{ab} pixel is settled with '1' that pixel is recognized as a noisy pixels whereas '0' means non-noisy pixel.

A 3×3 size window centred through q_{ab} is utilized to gather the neighbour elements depending on Equation (3),

$$W_{3 \times 3}^{n+1, m+1} = q_{a+n, b+m} \quad (3)$$

where

$$n \in \left[-\text{fix} \left(\frac{w_s}{2} \right), \text{fix} \left(\frac{w_s}{2} \right) \right] \quad (4)$$

$$m \in \left[-\text{fix} \left(\frac{w_s}{2} \right), \text{fix} \left(\frac{w_s}{2} \right) \right] \quad (5)$$

where the term $W_{3 \times 3}$ indicates the 3×3 size window, n represents the index for row indication, m denotes the e index for column indication and w_s represents the window size.

The noisy pixels count is calculated das window using Equation (6) as follows:

$$C_{Nq} = \begin{cases} C_{Nq} = C_{Nq+1}, \text{ if } w_{3 \times 3}^{n, m} = 0 \ \parallel \ w_{3 \times 3}^{n, m} = 255; \\ C_{Nq}; \end{cases} \quad (6)$$

where

$$n \in [0, w_s - 1] \quad (7)$$

$$m \in [0, w_s - 1] \quad (8)$$

where C_{Nq} indicates the noisy pixel count. The proposed ASMD-UTMF depends on the value of a pixel to be filtered. Hence, the input images with salt and pepper noise are preprocessed by ASMD-UTMF. Therefore, the ASMD-UTMF model has effectively pre-processed the input noisy image and provides more accurate images with reduced noises. To get a more accurate image the weight parameter Nq^{ab} and C_{Nq} of the ASMD-UTMF model are optimized using hybrid balancing composite motion optimization and forensic-based investigation algorithm (Hyb-BCO-FBIA). The hybrid balancing composite motion optimization and forensic-based investigation algorithm are explained below,

3.3. Step-wise process of hybrid balancing composite motion optimization and forensic-based investigation algorithm for optimizing hyperparameter of ASMD-UTMF

In this work, hybrid balancing composite motion optimization and forensic-based investigation algorithm (Hyb-BCO-FBIA) are exploited to enlarge the ASMD-UTMF for discovering the optimum parameters. Here, the Hyb-BCO-FBIA algorithm is utilized for tuning hyperparameters of ASMD-UTMF.

Generally, some systems are used for barrier generation, for instance, grid surveys, manual surveys and random surveys. Nevertheless, the thesis studies share their unusual weakness regarding the timing of reiteration. Thus, to overcome this problem, Hyb-BCO-FBIA is utilized.

Among the population-based optimization techniques are hybrid balancing composite motion optimization and Forensic-Based Inquiry Algorithm. The Hyb-BCO-FBIA algorithm is uncomplicated and devoid of any inherent characteristics. The solution space's classification as Cartesian serves as the driving force behind this. In fact, the candidate solution moves in close proximity to superior ones in order to explore the search space and take advantage of local regions. The highest-ranked person could consequently enhance their current local space or move to a new space in every era. A mathematical approach based on random testing is developed to control the progression characteristics of potential solutions. It probabilistically balances each person's investigations and exploitation searches and combines them into a composite. Population-seeking capability could be balanced throughout the optimization procedure if each individual equalizes its exploration with exploitation capabilities.

Since the Hyb-BCO-FBIA algorithm has an extensive range of control parameters and performs well in handling complicated problems in high dimensions, it was chosen for this manuscript. The Hyb-BCO-FBIA algorithm utilizes the ASMD-UTMF weight parameters Nq^{ab} and C_{Nq} of the ASMD-UTMF. For getting the optimal accurate image, Hyb-BCO-FBIA algorithm is utilized. The stepwise procedure of Hyb-BCO-FBIA algorithm is described below.

3.3.1. Step 1: initialization

The population distribution and forensic-based investigation is initialized uniformly on solution space utilizing the given Equation (9),

$$y_a = y_a^L + \text{rand}(1, d) \times (y_a^U - y_a^L) \quad (9)$$

where y_a^U and y_a^L indicates the lower, and upper boundaries of a^{th} the individual, $\text{rand}(1, d)$ indicates d dimensional vector fulfilling uniform distribution at $[0, 1]$ range.

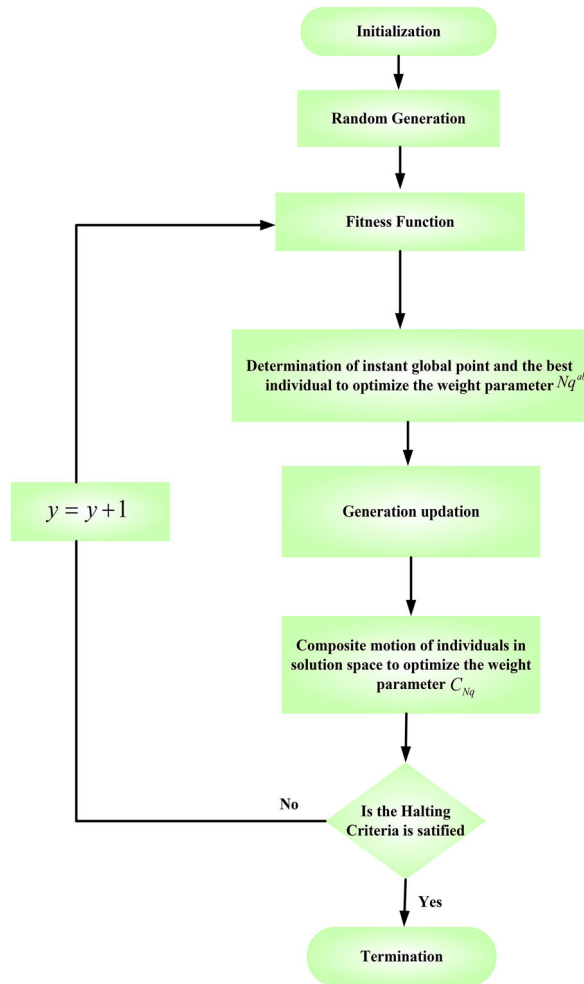


Figure 2. Flowchart for Hyb-BCO-FBIA algorithm.

3.3.2. Step 2: random generation

The input parameters are produced randomly after the process of initialization. Hence, the values of best fitness for each balancing composite motion optimization and forensic-based investigation algorithm are selected based on the explicit hyper-parameter situation. Figure 2 depicts the flowchart for Hyb-BCO-FBIA algorithm.

3.3.3. Step 3: fitness function

Generate the random solution through the initialized values. This solution is calculated and the goal function indicates the parameter value of optimization, like Nq^{ab} and C_{Nq} parameter and it is given in Equation (10),

$$\text{Fitness}_{\text{function}} = \text{Optimization}[Nq^{ab} \text{ and } C_{Nq}] \quad (10)$$

3.3.4. Step 4: determination of instant global point and best individual to optimize weight parameter Nq^{ab}

In Hyb-BCO-FBIA, the value of objective function based on the individuals are ranked in every generation. The Hyb-BCO-FBIA algorithm ranks individuals according to their objective function value throughout all generations. The NP ranked individual can be found at several local optimal locations in the S solution

space. Consider a^{th} individual in S on every generation, their absolute movement including related motion in terms of better b^{th} ranking ($b < a$ or $b = a = 1$) with the transportation motion of b^{th} individual depends on global optimization point as stated in Equation (11),

$$u_a = u_{a/b} + u_b \quad (11)$$

where $u_{a/b}$ represents a^{th} individual relative movement vector depends on b , u_a and u_b indicates the movement vectors.

3.3.5. Step 5: generation updation

Hyb-BCO-FBIA algorithm will experience fast convergence. Therefore, updated the global optimization point $G(O)$ in the t^{th} generation is expressed in Equation (12) as follows:

$$y_{G(O)}^t = y_1^{t-1} \quad (12)$$

The Best individual from the previous generation is indicated by y_1^{t-1} in Equation (12). Therefore, t^{th} stated in Equation (13) the updated global optimization point on generation is scaled via the selection amid the prior best y_1^{t-1} depending on its objective function values.

$$y_{G(O)}^t = \begin{cases} v_1^t; & \text{if } f(v_1^t) < f(y_1^{t-1}), \\ y_1^{t-1}; & \text{otherwise.} \end{cases} \quad (13)$$

where v_1^t represents the trial individual and it is computed by utilizing population information of the prior generation and is expressed in Equation (14) as follows:

$$v_1^t = v_c + v_{k_1/k_2}^t + v_{k_2/1}^t \quad (14)$$

where v_{k_1/k_2}^t and $v_{k_2/1}^t$ indicates the pseudo relative movements of the k_1^{th} individual, k_1 is randomly chosen at $[2, NP]$ range and v_c represents the centre point of design space $[LB, UB]$, it is exhibited in Equation (15) as follows:

$$v_c = \frac{LB + UB}{2} \quad (15)$$

However, the composite vector is replaced to the design space's centre point, because the design space has symmetrical depending on trial position created at the search space, the probability of feasible detection $G(O)$ by generations may increase.

3.3.6. Step 6: composite motion of individuals on solution space to optimize weight parameter C_{Nq}

Here, the a^{th} individual shift towards or away from better b^{th} including point $G(O)$. The probabilities of allocating positive, negative signs of $u_{a/b}$, u_b in local as well as global searches are equivalent to balance the exploration with exploitation capabilities of every individual at search space. The movement of global search

u_b is computed using Equation (16) as follows:

$$u_b = \beta_b(y_{G(O)} - y_b) \quad (16)$$

where β_b represents movement distance first-order derivative is measured using Equation (17) as follows:

$$\beta_b = S_G \times du_b \quad (17)$$

From Equation (17), S_G represents the global step size measuring the b^{th} individual movement and du_b represents the accuracy of image.

3.3.7. Step 7: termination

In termination, the optimum hyper-parameter Nq^{ab} and C_{Nq} are selected in ASMD-UTMF using hybrid balancing composite motion optimization and forensic-based investigation algorithm (Hyb-BCO-FBIA) alternatively repeat step 3 until the halting criteria $y = y + 1$ is met. At last, ASMD-UTMF provides the more accurate denoised image utilizing Hyb-BCO-FBIA algorithm.

4. Result and discussion

In this section describes the removal of salt and pepper noise with ASMD-UTMF optimized with hybrid balancing composite motion optimization and forensic-based investigation algorithm. Millions of scientists and engineers utilize the programming and numerical computing platform MATLAB to build models, design algorithms, and analyse information. The proposed work implementation is carried out by the MATLABR2019b platform. Here, the performance metrics like PSNR, IEF, MSE, SSIM, error rate, processing time, MAE and RMSE are analysed. Here the performance of the proposed is related to existing systems as de-noising of images as RSPN-HFGOA, RSPN-ANFIS, RSPN-APCNN-GWO and RSPN-DB-ATMWMF respectively.

4.1. Dataset description

The execution of removal of SPN for input images like boat-ocean-sea-water-sunset, boat-sea-inflatable-boat-coast, ferry-cargo-ship-carrier-the-barge-venicare taken from boat-types-recognition dataset. This dataset is used in a blog post where it trains an image recognition model through TensorFlow to find anything in images and videos. It contains about 1,500 images of ships, of several dimensions, but is categorized by dissimilar sorts: buoy, cruise ship, ferry, cargo ship, gondola, inflatable boat, kayak, paper boat and sailboat [13].

Cat-image-Domestic Long Hair, cat-image-Maine Coon and cat-image-Siberian are taken from the cat-breeds-dataset. This dataset contains images representing 67 dissimilar cat breeds. Over the years, contribute

additional pictures of rare or minority breeds to this. Advertisers, not experts, have designated these breeds; there is a chance of inaccuracy [14].

Car-road-Audi, img-road-Hyundai Creta, img-road-Toyota Innova are taken from cars-image-dataset. This dataset consists of various types of cars. The dataset is organized into 2 folders (train, test) and has subfolders for each car category. There are 4,165 images (JPG) and 7 classes of cars [15].

Butterfly-plant-img-ATALA, butterfly-plant-img-RED CRACKER, butterfly-plant-img-ORANGE TIP are taken from butterfly-images40-species dataset. All images are $224 \times 224 \times 3$ in jpg format. The train set has 9285 images partitioned into 75 subdirectories one for every species. The test set has 375 images partitioned into 75 sub-directories through 5 test images per species. The valid set has 375 images partitioned into 750 sub-directories through 5 validation images per species [16].

Girl-people-landscape-sun, Yellow-bellied-Flycatcher, bird-photo-Flamingo are taken from birds-200 dataset. 200 different bird species are represented in the image dataset (mainly North American). There are 6,003 bird photos in total, divided into 200 categories. For every image in the dataset, bounding boxes, approximate segmentation, and attribute data are also provided [17].

Figure 3 portrays output images of the removal of SPN. In this, input images are taken from the boat-types-recognition dataset, cat-breeds-dataset, cars-image-dataset, butterfly-images40-species dataset and birds-200 dataset. These input images contain several unwanted salt and pepper noises which affect the quality of the images and then the pictures are pre-processed for removing SPNs. Finally, it provides a denoised image.

4.2. Performance metrics

The performance metrics such as PSNR, IEF, MSE, Structural Similarity Index Measure (SSIM), error rate, processing time, Mean Absolute Error (MAE) and Root Mean Square Error (RMSE) are analysed. They are as follows.

4.2.1. Peak signal-to-noise ratio (PSNR)

PSNR is described as the ratio between signal variance and reconstruction error. PSNR is expressed in Equation (18) as follows:

$$\text{PSNR} = 10 \log_{10} \frac{255^2}{\frac{1}{M} \sum_{a,b} (r_{a,b} - x_{a,b})^2} \quad (18)$$

where M indicates the total number of image pixels, $r_{a,b}$ and $x_{a,b}$ indicates the levels of $q_{a,b}$ on restored image and original noise-free image, correspondingly.































Images	Input image with salt and pepper noise	Denoised Image	Image Size
boat-ocean-sea-water-sunset			350 × 553 × 3
boat-sea-inflatable-boat-coast			350 × 553 × 3
ferry-cargo-ship-carrier-the-barge-venic			350 × 554 × 3
cat-image-Domestic Long Hair			350 × 464 × 3
cat-image-Maine Coon			350 × 464 × 3
cat-image-Siberian			350 × 553 × 3
car-road-Audi			350 × 464 × 3
img-road-Hyundai Creta			350 × 464 × 3
img-road-Toyota Innova			350 × 464 × 3
butterfly-plant-ing-ATALA			350 × 553 × 3
butterfly-plant-ing-RED CRACKER			350 × 554 × 3
butterfly-plant-ing-ORANGE TIP			350 × 554 × 3
girl-people-landscape-sun			350 × 464 × 3
Yellow_bellied-Flycatcher			350 × 553 × 3
bird-photo-Flamingo			350 × 553 × 3

Figure 3. Output images of removal of salt and pepper noise.

4.2.2. Image enhancement factor (IEF)

The IEF measures the improvement quality of the denoising performance of an exact system by taking three parameters original image, noisy image, and denoised images. The image enhancement factor is calculated using Equation (19) as follows:

$$IEF = \frac{(\sum_a \sum_b |\eta(a, b) - x(a, b)|)^2}{(\sum_a \sum_b |r(a, b) - x(a, b)|)^2} \quad (19)$$

where $x(a, b)$ represents the original image, $r(a, b)$ refers restored image and η indicates noisy image.

4.2.3. Mean squared error (MSE)

MSE is defined as certain kind of average or sum of the square error among two images. The mean squared error is estimated using Equation (20) as follows:

$$MSE = \frac{1}{NM} \sum_{n=0}^{N-1} \sum_{m=0}^{M-1} [r_{a,b} - x_{a,b}]^2 \quad (20)$$

4.2.4. Structural similarity index measure (SSIM)

SSIM is calculated using Equation (21) as follows:

$$SSIM(L, M)$$

$$= \frac{1}{N} \sum_{b=1}^N \left(\frac{(2\mu_{lb}\mu_{mb} + C_1)(2\sigma_{lbmb} + C_2)}{(\mu_{lb}^2 + \mu_{mb}^2 + C_1)(\sigma_{lb}^2 + \sigma_{mb}^2 + C_2)} \right) \quad (21)$$

where L and M denote original noise-free and restored image, lb and mb represents image contents at local window, N indicates number of local windows, μ_{lb} and μ_{mb} indicates mean of lb and mb respectively, σ_{lb} and σ_{mb} represents the respective standard deviation, C_1 and C_2 represents the free parameter.

4.2.5. Mean absolute error (MAE)

MAE is described as the maximal absolute value between the original image and the degraded image. MAE is calculated using Equation (22) as follows:

$$MAE = \frac{1}{NM} \sum_{a,b} |r_{a,b} - x_{a,b}| \quad (22)$$

Equation (22), $r_{a,b}$ and $x_{a,b}$ denotes the pixel values of the restored image and original image.

4.2.6. Root mean square error (RMSE)

RMSE is described as the square root of mean square error and is expressed in Equation (23) as follows:

$$RMSE = \sqrt{MSE} \quad (23)$$

4.2.7. Normalized correlation (NC)

NC is a measure of the difference between a denoised image W_N and an original image W . NC is considered as using Equation (24) as follows:

$$NC(W, W_N) = \frac{\sum_{i=1}^N \sum_{j=1}^M [W(i,j) - \mu_1] [W_N(i,j) - \mu_2]}{\sqrt{\sum_{i=1}^N \sum_{j=1}^M [W(i,j) - \mu_1]^2} \sqrt{\sum_{i=1}^N \sum_{j=1}^M [W_N(i,j) - \mu_2]^2}} \quad (24)$$

where μ_1 and μ_2 refers mean values of W and W_N correspondingly, If original and denoised image closely resemble one another $NC \approx 1$. In the case wherever $NC = 1$, the original and denoised images are equal.

4.3. Performance analysis

Figure 4–12 represents the simulation result of the removal of salt and pepper noise with ASMD-UTMF optimized with hybrid balancing composite motion optimization and forensic-based investigation algorithm. Here the performance metrics of PSNR, MSE, SSIM, MAE, error rate, processing time, Normalized correlation and RMSE are analysed and compared with existing methods like RSPN-HFGOA, RSPN-ANFIS, RSPN-APCNN-GWO and RSPN-DB-ATMWMF respectively.

Figure 4 shows the performance analysis of PSNR. Here the performance of the proposed RSPN-ASMD-UTMF-Hyb-BCO-FBIA system is related to existing systems like RSPN-HFGOA, RSPN-ANFIS, RSPN-APCNN-GWO and RSPN-DB-ATMWMF. For noise density of 10%, the proposed RSPN-ASMD-UTMF-Hyb-BCO-FBIA method provides 23.6%, 35.66%, 27.65% and 25.64% higher PSNR compared with existing methods like RSPN-HFGOA, RSPN-ANFIS, RSPN-APCNN-GWO and RSPN-DB-ATMWMF respectively. For noise density of 20%, the proposed RSPN-ASMD-UTMF-Hyb-BCO-FBIA method provides 24.5%, 19.09%, 21.5%, and 24.6% higher PSNR related with existing systems as RSPN-HFGOA, RSPN-ANFIS, RSPN-APCNN-GWO and RSPN-DB-ATMWMF respectively. For noise density of 30%, the proposed RSPN-ASMD-UTMF-Hyb-BCO-FBIA method provides 18.9%, 23.4%, 17.9%, and 29.8% higher PSNR related with existing systems as RSPN-HFGOA, RSPN-ANFIS, RSPN-APCNN-GWO and RSPN-DB-ATMWMF respectively. For noise density of 40%, the proposed RSPN-ASMD-UTMF-Hyb-BCO-FBIA method provides 20.9%, 30.9%, 27.8%, and 13.5% higher PSNR compared with existing methods like RSPN-HFGOA, RSPN-ANFIS, RSPN-APCNN-GWO and RSPN-DB-ATMWMF respectively. For noise density of 50%, the proposed RSPN-ASMD-UTMF-Hyb-BCO-FBIA method provides 19.06%, 29.09%, 23.8%, and 20.5% higher PSNR compared with existing methods like RSPN-HFGOA, RSPN-ANFIS, RSPN-APCNN-GWO and RSPN-DB-ATMWMF respectively.

Figure 5 portrays an analysis of the image enhancement factor (IEF). Here the performance of the proposed RSPN-ASMD-UTMF-Hyb-BCO-FBIA method is compared with existing methods like RSPN-HFGOA, RSPN-ANFIS, RSPN-APCNN-GWO and RSPN-DB-ATMWMF. For noise density of 10%, the proposed RSPN-ASMD-UTMF-Hyb-BCO-FBIA method provides 29%, 19.96%, 24.69%, and 17.9% higher IEF related with existing systems as RSPN-HFGOA, RSPN-ANFIS, RSPN-APCNN-GWO and RSPN-DB-ATMWMF respectively. For noise density of 20%, the proposed RSPN-ASMD-UTMF-Hyb-BCO-FBIA method provides 28.7%, 18.65%, 23.64% and 18.34% higher IEF compared with existing methods like RSPN-HFGOA, RSPN-ANFIS, RSPN-APCNN-GWO and RSPN-DB-ATMWMF respectively. For noise density of 30%, the proposed RSPN-ASMD-UTMF-Hyb-BCO-FBIA method provides 23.5%, 18.6%, 21.9%, and 15.7% higher IEF compared with existing methods like RSPN-HFGOA, RSPN-ANFIS, RSPN-APCNN-GWO and RSPN-DB-ATMWMF respectively. For noise density of 40%, the proposed RSPN-ASMD-UTMF-Hyb-BCO-FBIA method provides 28.9%, 23.4%, 26.7%, and 22.8% higher IEF compared with existing methods like RSPN-HFGOA, RSPN-ANFIS, RSPN-APCNN-GWO

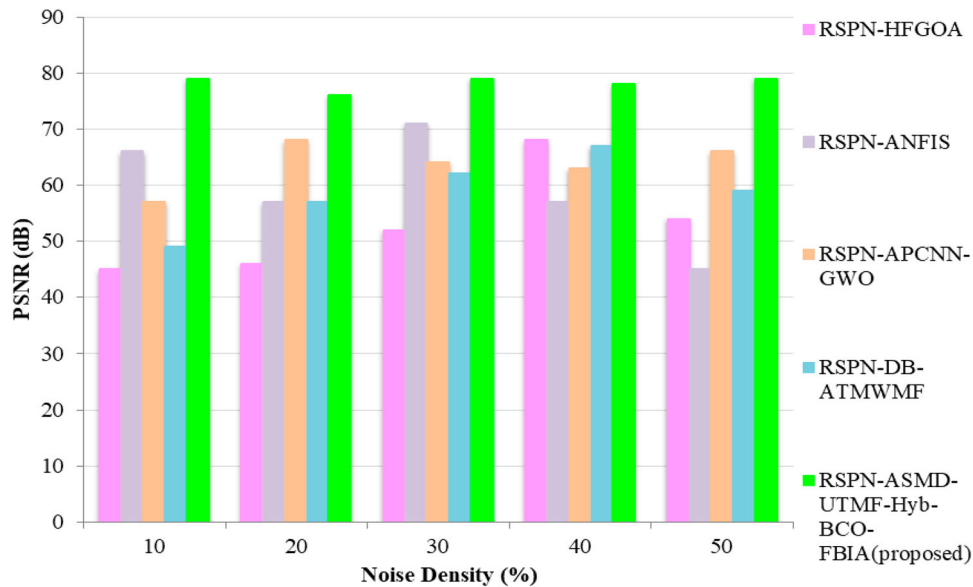


Figure 4. Performance analysis of peak signal-to-noise ratio (PSNR).

and RSPN-DB-ATMWMF respectively. For noise density of 50%, the proposed RSPN-ASMD-UTMF-Hyb-BCO-FBIA method provides 29.8%, 17.8%, 28.79%, and 24.7% higher IEF compared with existing methods like RSPN-HFGOA, RSPN-ANFIS, RSPN-APCNN-GWO and RSPN-DB-ATMWMF respectively.

Figure 6 shows a performance analysis of mean squared error (MSE). Here the performance of the proposed RSPN-ASMD-UTMF-Hyb-BCO-FBIA system is related to existing systems like RSPN-HFGOA, RSPN-ANFIS, RSPN-APCNN-GWO and RSPN-DB-ATMWMF. For noise density of 10%, the proposed RSPN-ASMD-UTMF-Hyb-BCO-FBIA method provides 25.6%, 19.87%, 13.64%, and 18.7% lower MSE compared with existing methods like RSPN-HFGOA, RSPN-ANFIS, RSPN-APCNN-GWO and RSPN-DB-ATMWMF respectively. For noise density of 20%, the proposed RSPN-ASMD-UTMF-Hyb-BCO-FBIA method provides 25.7%, 28.5%, 12.8%, and 25.76% lower MSE compared with existing methods like RSPN-HFGOA, RSPN-ANFIS, RSPN-APCNN-GWO and RSPN-DB-ATMWMF respectively. For noise density of 30%, the proposed RSPN-ASMD-UTMF-Hyb-BCO-FBIA method provides 24.75%, 23.84%, 20.6%, and 29.75% lower MSE related with existing systems as RSPN-HFGOA, RSPN-ANFIS, RSPN-APCNN-GWO and RSPN-DB-ATMWMF respectively. For noise density of 40%, the proposed RSPN-ASMD-UTMF-Hyb-BCO-FBIA method provides 29.8%, 14.7%, 18.9%, and 21.5% lower MSE compared with existing methods like RSPN-HFGOA, RSPN-ANFIS, RSPN-APCNN-GWO and RSPN-DB-ATMWMF respectively. For noise density of 50%, the proposed RSPN-ASMD-UTMF-Hyb-BCO-FBIA method provides 25.6%, 27.8%, 26.7%, and 23.6% lower MSE compared with existing methods like RSPN-HFGOA, RSPN-ANFIS, RSPN-APCNN-GWO and RSPN-DB-ATMWMF respectively.

Figure 7 shows the performance of the Structural similarity index measure (SSIM). The proposed RSPN-ASMD-UTMF-Hyb-BCO-FBIA method is compared with existing methods like RSPN-HFGOA, RSPN-ANFIS, RSPN-APCNN-GWO and RSPN-DB-ATMWMF. For noise density of 10%, the proposed RSPN-ASMD-UTMF-Hyb-BCO-FBIA method provides 33.34%, 32.74%, 22.46%, and 38.46% higher SSIM compared with existing methods like RSPN-HFGOA, RSPN-ANFIS, RSPN-APCNN-GWO and RSPN-DB-ATMWMF respectively. For noise density of 20%, the proposed RSPN-ASMD-UTMF-Hyb-BCO-FBIA method provides 27.48%, 32.53%, 22.94% and 30.83% higher SSIM compared with existing methods like RSPN-HFGOA, RSPN-ANFIS, RSPN-APCNN-GWO, RSPN-DB-ATMWMF respectively. For noise density of 30%, the proposed RSPN-ASMD-UTMF-Hyb-BCO-FBIA method provides 19.54%, 12.63%, 27.37%, and 28.36% higher SSIM compared with existing methods like RSPN-HFGOA, RSPN-ANFIS, RSPN-APCNN-GWO and RSPN-DB-ATMWMF respectively. For noise density of 40%, the proposed RSPN-ASMD-UTMF-Hyb-BCO-FBIA method provides 14.85%, 22.85%, 28.46%, and 35.82% higher SSIM compared with existing methods like RSPN-HFGOA, RSPN-ANFIS, RSPN-APCNN-GWO and RSPN-DB-ATMWMF respectively. For noise density 50%, the proposed RSPN-ASMD-UTMF-Hyb-BCO-FBIA method provides 18.03%, 28.64%, 30.72%, and 33.74% higher SSIM compared with existing methods like RSPN-HFGOA, RSPN-ANFIS, RSPN-APCNN-GWO and RSPN-DB-ATMWMF respectively.

Figure 8 shows the performance analysis of mean absolute error (MAE). The proposed RSPN-ASMD-UTMF-Hyb-BCO-FBIA method is compared with existing methods like RSPN-HFGOA, RSPN-ANFIS, RSPN-APCNN-GWO and RSPN-DB-ATMWMF. For

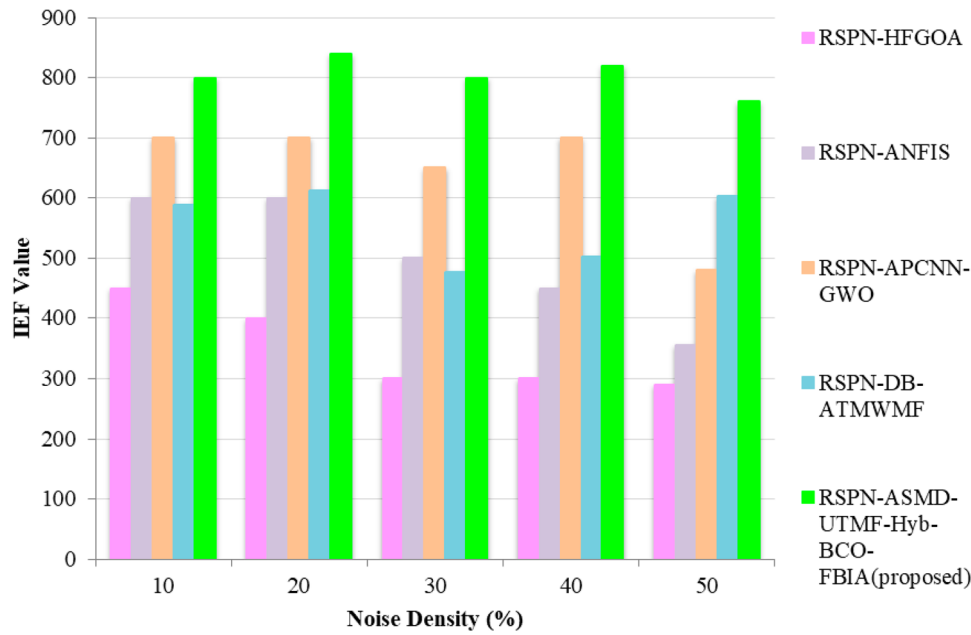


Figure 5. Performance analysis of image enhancement factor (IEF).

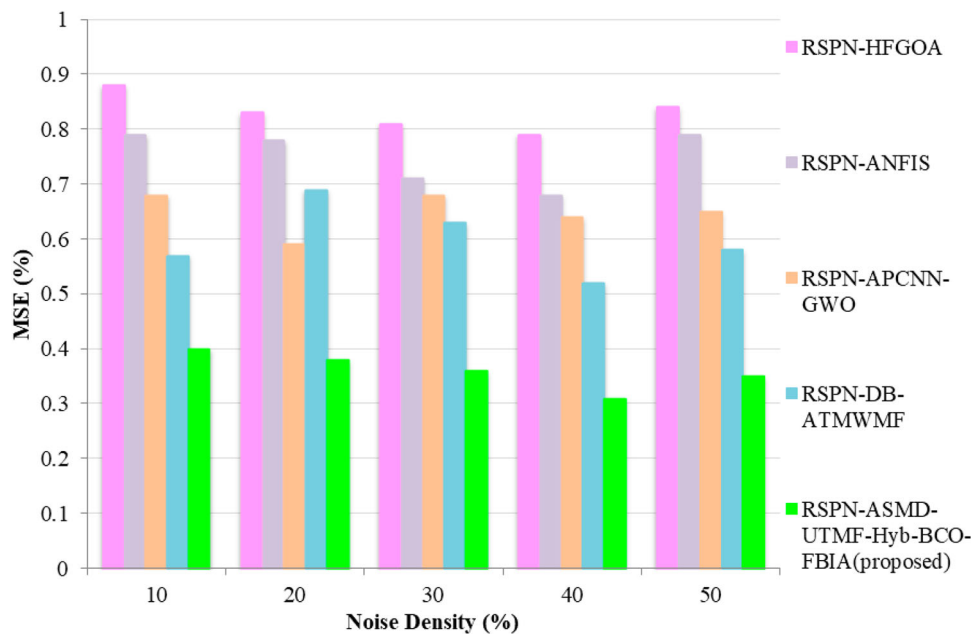


Figure 6. Performance analysis of mean squared error (MSE).

noise density of 10%, the proposed RSPN-ASMD-UTMF-Hyb-BCO-FBIA method provides 25.93%, 28.94%, 20.83%, and 33.02% lower MAE compared with existing methods like RSPN-HFGOA, RSPN-ANFIS, RSPN-APCNN-GWO and RSPN-DB-ATMWMF respectively. For noise density of 20%, the proposed RSPN-ASMD-UTMF-Hyb-BCO-FBIA method provides 35.74%, 26.73%, 27.83% and 19.82% lower MAE compared with existing methods like RSPN-HFGOA, RSPN-ANFIS, RSPN-APCNN-GWO, RSPN-DB-ATMWMF respectively. For noise density of 30%, the proposed RSPN-ASMD-UTMF-Hyb-BCO-FBIA method provides 21.83%, 26.83%, 36.48%, and 11.93% lower MAE compared with existing methods

like RSPN-HFGOA, RSPN-ANFIS, RSPN-APCNN-GWO and RSPN-DB-ATMWMF respectively. For noise density of 40%, the proposed RSPN-ASMD-UTMF-Hyb-BCO-FBIA method provides 28.43%, 28.46%, 39.56%, and 28.56% lower MAE compared with existing methods like RSPN-HFGOA, RSPN-ANFIS, RSPN-APCNN-GWO and RSPN-DB-ATMWMF respectively. For noise density of 50%, the proposed RSPN-ASMD-UTMF-Hyb-BCO-FBIA method provides 15.86%, 22.94%, 14.86%, and 17.35% lower MAE compared with existing methods like RSPN-HFGOA, RSPN-ANFIS, RSPN-APCNN-GWO and RSPN-DB-ATMWMF respectively.

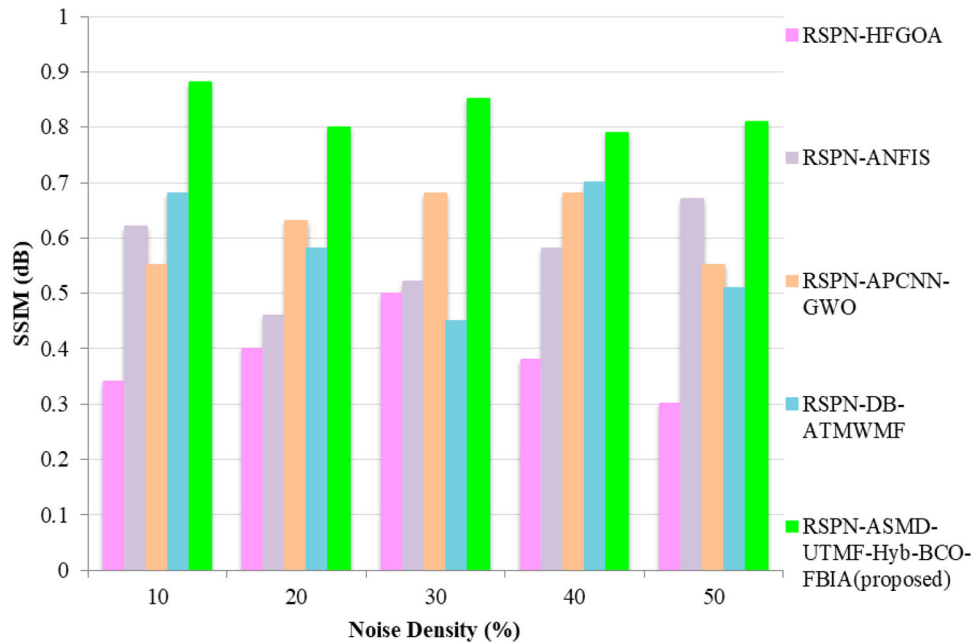


Figure 7. Performance analysis of structural similarity index measure (SSIM).

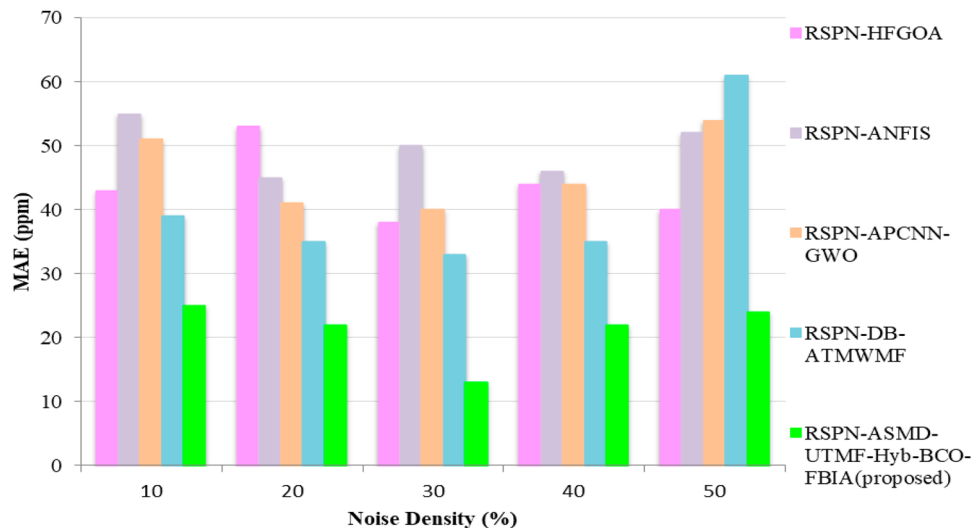


Figure 8. Performance analysis of mean absolute error (MAE).

Figure 9 shows an analysis of the error rate. Here the performance of the proposed RSPN-ASMD-UTMF-Hyb-BCO-FBIA method is related to existing systems as RSPN-HFGOA, RSPN-ANFIS, RSPN-APCNN-GWO and RSPN-DB-ATMWMF. For noise density of 10%, the proposed RSPN-ASMD-UTMF-Hyb-BCO-FBIA method provides 21.84%, 23.94%, 18.74%, and 32.84% lower error rates compared with existing methods like RSPN-HFGOA, RSPN-ANFIS, RSPN-APCNN-GWO and RSPN-DB-ATMWMF respectively. For noise density of 20%, the proposed RSPN-ASMD-UTMF-Hyb-BCO-FBIA method provides 32.94%, 21.84%, 20.84% and 14.73% lower error rates compared with existing methods like RSPN-HFGOA, RSPN-ANFIS, RSPN-APCNN-GWO and RSPN-DB-ATMWMF respectively. For noise density of 30%, the proposed RSPN-ASMD-UTMF-Hyb-BCO-FBIA method provides 19.73%, 13.84%, 28.47%,

and 24.75% lower error rates compared with existing methods like RSPN-HFGOA, RSPN-ANFIS, RSPN-APCNN-GWO and RSPN-DB-ATMWMF respectively. For noise density of 40%, the proposed RSPN-ASMD-UTMF-Hyb-BCO-FBIA method provides 23.84%, 11.83%, 27.58%, and 21.95% lower error rates compared with existing methods like RSPN-HFGOA, RSPN-ANFIS, RSPN-APCNN-GWO and RSPN-DB-ATMWMF respectively. For noise density of 50%, the proposed RSPN-ASMD-UTMF-Hyb-BCO-FBIA method provides 28.39%, 17.04%, 18.46%, and 19.35% lower error rates compared with existing methods like RSPN-HFGOA, RSPN-ANFIS, RSPN-APCNN-GWO and RSPN-DB-ATMWMF correspondingly.

Figure 10 portrays the performance analysis of processing time. Here the performance of the proposed RSPN-ASMD-UTMF-Hyb-BCO-FBIA system is related to existing systems as RSPN-HFGOA,

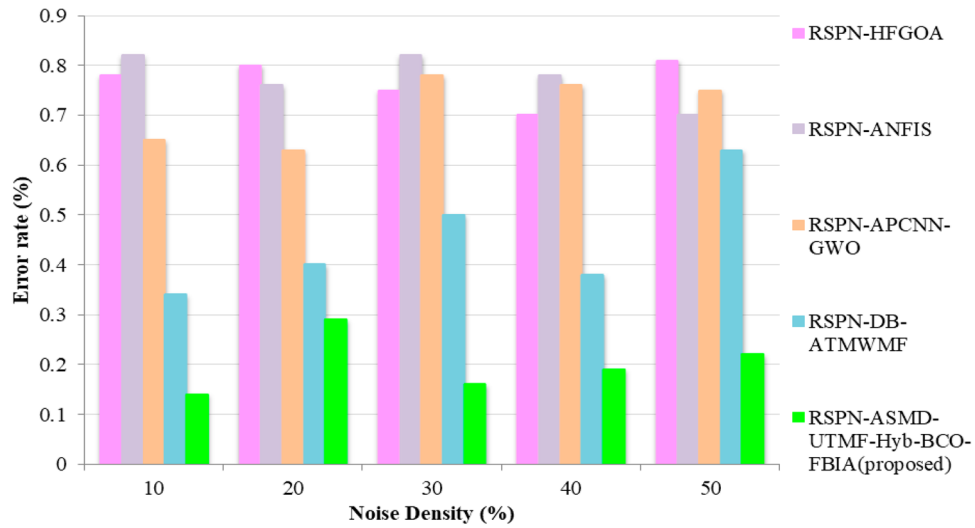


Figure 9. Analysis of error rate.

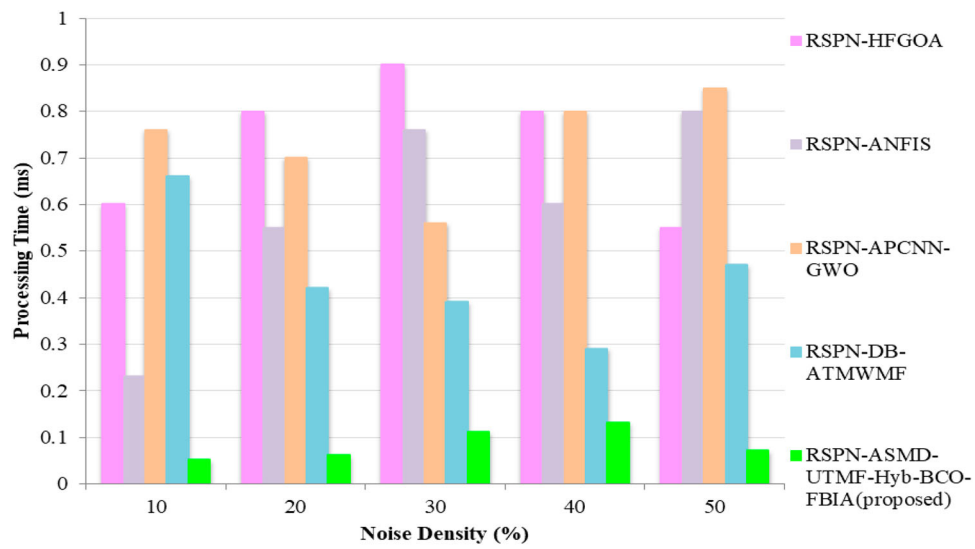


Figure 10. Performance analysis of processing time.

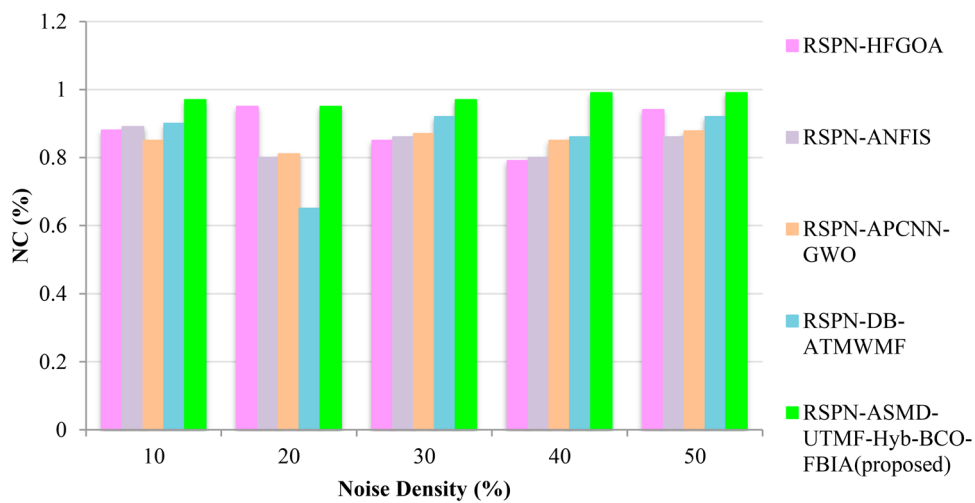


Figure 11. Performance analysis of normalized correlation (NC).

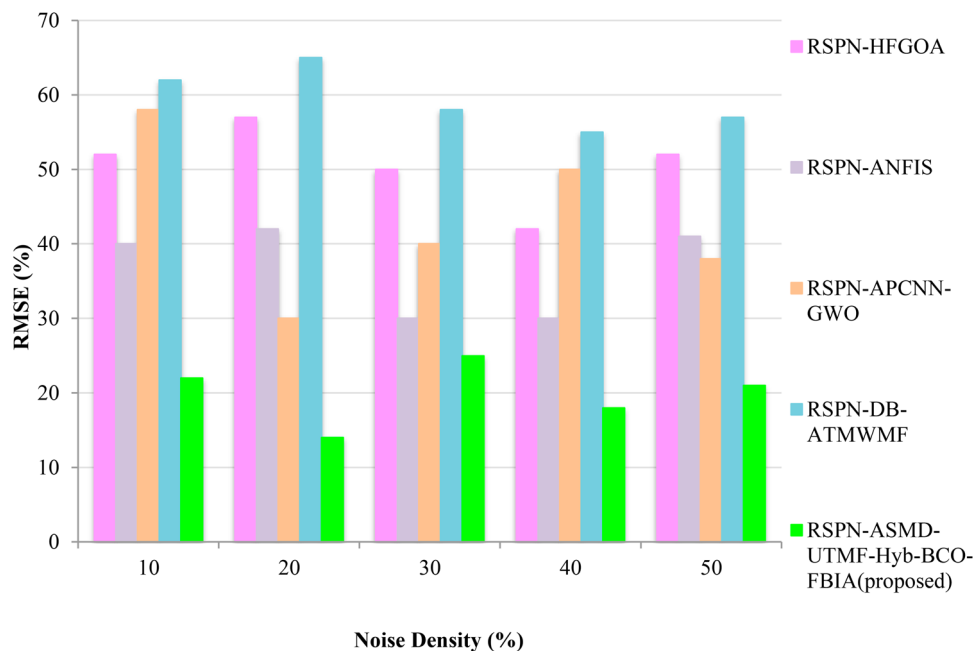


Figure 12. Performance analysis of root mean square error (RMSE).

RSPN-ANFIS, RSPN-APCNN-GWO and RSPN-DB-ATMWMF. For noise density of 10%, the proposed RSPN-ASMD-UTMF-Hyb-BCO-FBIA method provides 18.46%, 12.64%, 16.48%, and 34.85% lower processing time compared with existing methods like RSPN-HFGOA, RSPN-ANFIS, RSPN-APCNN-GWO and RSPN-DB-ATMWMF respectively. For noise density of 20%, the proposed RSPN-ASMD-UTMF-Hyb-BCO-FBIA method provides 35.84%, 29.85%, 27.46% and 17.46% lower processing time compared with existing methods like RSPN-HFGOA, RSPN-ANFIS, RSPN-APCNN-GWO and RSPN-DB-ATMWMF respectively. For noise density of 30%, the proposed RSPN-ASMD-UTMF-Hyb-BCO-FBIA method provides 15.78%, 16.97%, 28.56%, and 22.84% lower processing time compared with existing methods like RSPN-HFGOA, RSPN-ANFIS, RSPN-APCNN-GWO and RSPN-DB-ATMWMF respectively. For noise density of 40%, the proposed RSPN-ASMD-UTMF-Hyb-BCO-FBIA method provides 18.45%, 16.94%, 31.85% and 36.48% lower processing time compared with existing methods like RSPN-HFGOA, RSPN-ANFIS, RSPN-APCNN-GWO and RSPN-DB-ATMWMF respectively. For noise density of 50%, the proposed RSPN-ASMD-UTMF-Hyb-BCO-FBIA method provides 26.85%, 15.38%, 12.56% and 24.69% lower processing time compared with existing methods like RSPN-HFGOA, RSPN-ANFIS, RSPN-APCNN-GWO and RSPN-DB-ATMWMF respectively.

Figure 11 shows the performance analysis of Normalized Correlation (NC). Here the performance of the proposed RSPN-ASMD-UTMF-Hyb-BCO-FBIA method is compared with existing methods like RSPN-HFGOA, RSPN-ANFIS, RSPN-APCNN-GWO and RSPN-DB-ATMWMF. For noise density of 10%,

the proposed RSPN-ASMD-UTMF-Hyb-BCO-FBIA method provides 42.3%, 33.6%, 52.7% and 44.6% higher NC related with existing systems as RSPN-HFGOA, RSPN-ANFIS, RSPN-APCNN-GWO, RSPN-DB-ATMWMF respectively. For noise density of 20%, the proposed RSPN-ASMD-UTMF-Hyb-BCO-FBIA method provides 25.9%, 47.7%, 49.8%, and 68.2% higher NC compared with existing systems as RSPN-HFGOA, RSPN-ANFIS, RSPN-APCNN-GWO, RSPN-DB-ATMWMF respectively. For noise density of 30%, the proposed RSPN-ASMD-UTMF-Hyb-BCO-FBIA method provides 14.64%, 23.11%, 25.34%, and 18.81% higher NC compared with existing methods like RSPN-HFGOA, RSPN-ANFIS, RSPN-APCNN-GWO and RSPN-DB-ATMWMF respectively. For noise density of 40%, the proposed RSPN-ASMD-UTMF-Hyb-BCO-FBIA method provides 61.818%, 64.11%, 40.93% and 21.16% higher NC compared with existing methods like RSPN-HFGOA, RSPN-ANFIS, RSPN-APCNN-GWO, RSPN-DB-ATMWMF respectively. For noise density of 50%, the proposed RSPN-ASMD-UTMF-Hyb-BCO-FBIA method provides 41.23%, 67.62%, 47.22% and 19.17% higher NC compared with existing methods like RSPN-HFGOA, RSPN-ANFIS, RSPN-APCNN-GWO, RSPN-DB-ATMWMF respectively.

Figure 12 shows the performance analysis of root mean square error (RMSE). The proposed RSPN-ASMD-UTMF-Hyb-BCO-FBIA method is compared with existing methods like RSPN-HFGOA, RSPN-ANFIS, RSPN-APCNN-GWO and RSPN-DB-ATMWMF. For noise density of 10%, the proposed RSPN-ASMD-UTMF-Hyb-BCO-FBIA method provides 12.32%, 69.18%, 52.91% and 21.85% lower RMSE compared with existing methods like RSPN-HFGOA, RSPN-ANFIS, RSPN-APCNN-GWO and

RSPN-DB-ATMWMF respectively. For noise density of 20%, the proposed RSPN-ASMD-UTMF-Hyb-BCO-FBIA method provides 18.77%, 65.17%, 53.829% and 28.333% lower RMSE compared with existing methods like RSPN-HFGOA, RSPN-ANFIS, RSPN-APCNN-GWO, RSPN-DB-ATMWMF respectively. For noise density of 30%, the proposed RSPN-ASMD-UTMF-Hyb-BCO-FBIA method provides 19.87%, 11.49%, 24.5%, and 49.23% lower RMSE compared with existing methods like RSPN-HFGOA, RSPN-ANFIS, RSPN-APCNN-GWO, RSPN-DB-ATMWMF respectively. For noise density of 40%, the proposed RSPN-ASMD-UTMF-Hyb-BCO-FBIA method provides 35.08%, 17.77%, 71.43%, and 75% lower RMSE compared with existing methods RSPN-HFGOA, RSPN-ANFIS, RSPN-APCNN-GWO, RSPN-DB-ATMWMF respectively. For noise density of 50%, the proposed RSPN-ASMD-UTMF-Hyb-BCO-FBIA method provides 42.94%, 12.89%, 36.59%, and 51.43% lower RMSE compared with existing methods like RSPN-HFGOA, RSPN-ANFIS, RSPN-APCNN-GWO and RSPN-DB-ATMWMF respectively.

5. Conclusion

In this manuscript, the removal of salt and pepper noise with ASMD-UTMF optimized with hybrid balancing composite motion optimization and forensic-based investigation algorithm (R-SPN-ASMD-UTMF-Hyb-BCO-FBIA) is proposed. Initially, input images are taken from datasets such as the boat-types-recognition dataset, cat-breeds-dataset, cars-image-dataset, butterfly-images 40-species dataset and birds-200 dataset. Then images are pre-processed using an ASMD-UTMF filter. ASMD-UTMF does not expose any adoption of optimization systems to calculate the optimal parameters. Therefore, Hyb-BCO-FBIA is utilized to optimize the weight parameters of ASMD-UTMF. The proposed RSPN-ASMD-UTMF-Hyb-BCO-FBIA technique is executed on the MATLAB platform. Here, performance metrics such as PSNR, IEF, MSE, SSIM, error rate, processing time, MAE, RMSE, NC used for evaluation. The proposed R-SPN-ASMD-UTMF-Hyb-BCO-FBIA method attains lower RMSE of 95.75%, 97.64%, 94.64% and 91.23% compared with existing methods like RSPN-HFGOA, RSPN-ANFIS, RSPN-APCNN-GWO and RSPN-DB-ATMWMF respectively.

Disclosure statement

No potential conflict of interest was reported by the author(s).

References

- [1] Shi B, Gu F, Pang ZF, et al. Remove the salt and pepper noise based on the high order total variation and the nuclear norm regularization. *Appl Math Comput.* 2022;421:1–17.
- [2] Jyotiyana M, Kesswani N, Agarwal A. An improved approach for removal of salt and pepper noise in MR images. *Adv Deep Learn Artif Intell Rob. LNSS,* 2022;249:111–118.
- [3] Ebrahimnejad J, Naghsh A. Adaptive removal of high-density salt-and-pepper noise (ARSPN) for robust ROI detection used in watermarking of MRI images of the brain. *Comput Biol Med.* 2021;137:1–9. doi:10.1016/j.compbio.2021.104831
- [4] Sen AP, Rout NK. Probabilistic decision based improved trimmed median filter to remove high-density salt and pepper noise. *Pattern Recognit Image Anal.* 2020;30(3):401–415. doi:10.1134/S1054661820030244
- [5] Sheela CJJ, Suganthi G. An efficient denoising of impulse noise from MRI using adaptive switching modified decision based unsymmetric trimmed median filter. *Biomed Signal Process Control.* 2020;55:1–12.
- [6] Shaheen AM, Ginidi AR, El-Sehiemy RA, et al. A forensic-based investigation algorithm for parameter extraction of solar cell models. *IEEE Access.* 2020;9:1–20. doi:10.1109/ACCESS.2020.3046536
- [7] Le-Duc T, Nguyen QH, Nguyen-Xuan H. Balancing composite motion optimization. *Inf Sci (Ny).* 2020;520:250–270. doi:10.1016/j.ins.2020.02.013
- [8] Senthilselvi A, Duella J, Prabavathi R, et al. Performance evaluation of adaptive neuro fuzzy system (ANFIS) over fuzzy inference system (FIS) with optimization algorithm in de-noising of images from salt and pepper noise. *J Ambient Intell Humaniz Comput.* 2021;2020 a,b:1–6.
- [9] Kiruban M, Jayamani R, Ramu P. Removal of salt and pepper noise from SAR images using optimized APCNN in shearlet transform domain. *Arabian J Geosci.* 2021;14(6):1–10. doi:10.1007/s12517-021-06875-0
- [10] Christo MS, Vasanth K, Varatharajan R. A decision based asymmetrically trimmed modified winsorized median filter for the removal of salt and pepper noise in images and videos. *Multimed Tools Appl.* 2020;79(1):415–432. doi:10.1007/s11042-019-08124-9
- [11] Sharma N, Sohi PJS, Garg B, et al. A novel multilayer decision based iterative filter for removal of salt and pepper noise. *Multimed Tools Appl.* 2021;80(17):26531–26545. doi:10.1007/s11042-021-10958-1
- [12] Zhang H, Zhu Y, Zheng H. NAMF: a nonlocal adaptive mean filter for removal of salt-and-pepper noise. *Math Probl Eng.* 2021;2021:1–10.
- [13] <https://www.kaggle.com/datasets/clorichel/boat-types-recognition>
- [14] <https://www.kaggle.com/datasets/kshitij192/cars-image-dataset>
- [15] <https://www.kaggle.com/datasets/ma7555/cat-breeds-dataset>
- [16] <https://www.kaggle.com/datasets/gpiosenska/butterfly-images40-species>
- [17] <https://www.kaggle.com/datasets/dmccgow/birds-200>